

DESIGN AND DEVELOPMENT OF THE BEAMLINE SYSTEM FOR A PROTON THERAPY FACILITY *

B. Qin[†], W.J. Han, X. Liu, Z.F. Zhao, Q.S. Chen, Z.K. Liang, K.F. Liu, D. Li, J. Yang, M.W. Fan
Institute of Applied Electromagnetic Engineering,
Huazhong University of Science and Technology (HUST), Wuhan 430074, China

Abstract

A proton therapy facility with multiple treatment rooms based on superconducting cyclotron scheme is under development in HUST (Huazhong University of Science and Technology). Design features and overview of development progress for the beamline system will be presented in this paper, which mainly focuses on prototype beamline magnets, a kicker magnet for fast beam switch, and the gantry beamline using image optics.

INTRODUCTION

In last three decades, proton therapy (PT) has become an effective radio-therapy method for cancer treatment. Compared to X-ray or photon therapy, proton beam has a controllable depth-dose distribution with so called 'Bragg Peak' characteristic.

In HUST, a multiple treatment rooms proton therapy facility is under development [1], as shown in Fig. 1.

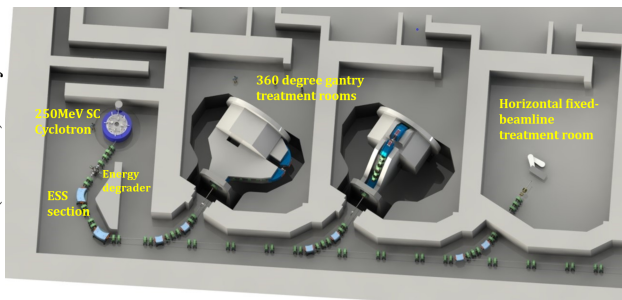


Figure 1: Overview of HUST-PTF.

The beamline system consists of an ESS (energy selection system) section, one horizontal fixed beamline and two 360 degree gantry beamlines connected by switch and period sections. Beamline optics has been designed with Transport [1, 2], and validated with COSY INFINITY [3]. Figure 2 shows the beam envelope fitted with Transport. Technical design for beamline magnets and energy degrader has been accomplished, manufacture and test are undergoing [4, 5].

PROTOTYPE MAGNETS AND FIELD MEASUREMENT

Three prototype magnets in the main beamline have been designed, manufactured and tested. Figure 3 shows these

Table 1: Parameters of Prototype Magnets

Magnet	Specification
L270	Aperture: 80 mm
Quadrupole	Max. gradient: 18.0 T/m Effective length: 270 mm Integral field harmonics: ≤ 5 units
30° Dipole	Central magnetic field: 0.82-1.62 T Entrance / exit edge angle: 15° Integral field homogeneity: $\leq \pm 0.1\%$
60° Dipole	± 180 degree, normal conducting Entrance / exit edge angle: 30° Integral field homogeneity: $\leq \pm 0.1\%$

magnets (one quadrupole and two dipoles), and specifications are listed in Table 1.

Two dipole magnets were measured by Hall probe, and the integral magnetic fields were measured by a long search coil measurement system. For operation field range 0.82 - 1.62 T corresponding to the proton energy 70 - 250 MeV, the integral field homogeneity in the good field region ± 40 mm is within $\pm 0.08\%$. Figure 4 shows the measured results of the 30° dipole. A rotation coil multipoles measurement system was applied to measure the L270 quadrupole, and Fig. 5 shows the measured results corresponding to three working currents. All magnet specifications have been fulfilled.

KICKER FOR FAST BEAM SWITCH

A kicker magnet will be installed at the downstream of the cyclotron, and before the energy degrader, for the purpose of fast beam switch during spot scanning. The main specifications are 100 μ s for rise and fall time with a maximum repetition rate 500 Hz, and the integral field is 0.025 T.m (1100 Gs for central field) which corresponds to the deflecting angle 10.4 mrad for 250 MeV proton beam.

A comparative study for the kicker core using soft ferrite and laminated steel materials was performed, with OPERA-3D TOSCA and ELEKTRA/TR solvers [6]. Both materials can meet the specification of static field. But for dynamic response in terms of hysteresis effect, laminated steel core shows non-neglectable lagging due to eddy currents, as illustrated in Fig. 6. Based on this, MnZn ferrite with saturation field 5350 Gs was chosen as the kicker core.

Figure 7 (a) shows the assemble view of the kicker with window frame. Figure 7 (b) shows the core assemble using 6 MnZn ferrite blocks. To avoid eddy currents, a ceramic

* This work was supported by The National Key Research and Development Program of China, with grant No. 2016YFC0105305; and by National Natural Science Foundation of China (11375068).

[†] bin.qin@mail.hust.edu.cn

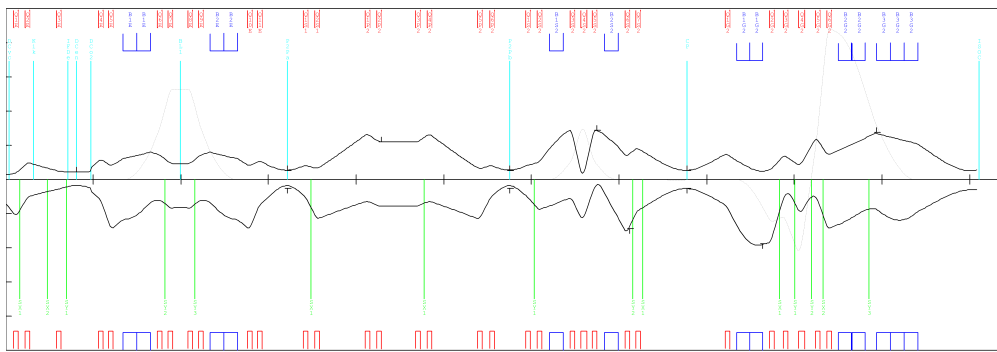


Figure 2: 1σ beam ($\epsilon = 7\pi$, $\delta p/p = \pm 0.3\%$) envelope, including ESS, period and gantry beamline.



Figure 3: Three prototype magnets, from left to right: (a) 60° dipole; (b) L270 mm quadrupole; (c) 30° dipole.

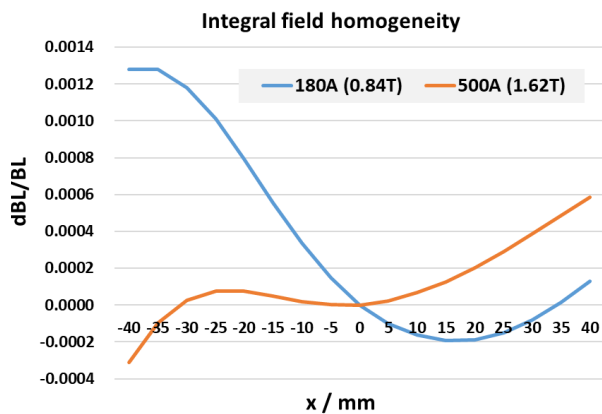


Figure 4: Integral field homogeneity of 30° dipole, operation current 180 A for 0.84 T central magnetic field and 500 A for 1.62 T were measured.

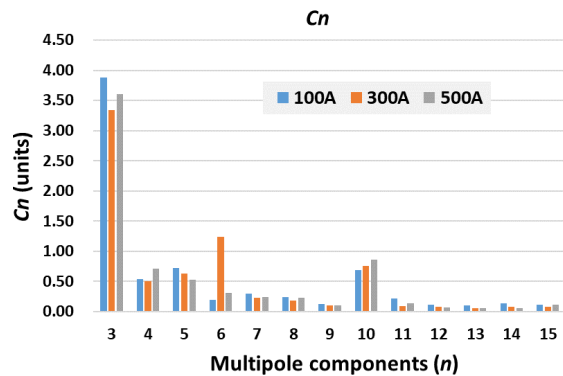


Figure 5: Measured multipole components ($n \geq 3$) of L270 quadrupole, operation current 100A (3.6T/m), 300A (10.8T/m) and 500A (17.8T/m) were measured.

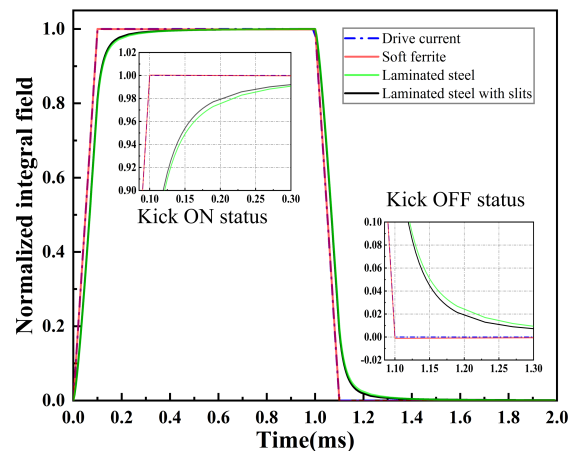


Figure 6: Hysteresis effect of the integral field, with 3 comparative models.

This is a preprint — the final version is published with IOP

vacuum chamber is chosen with a racetrack cross-section, as shown in Fig. 7 (c). The overall length of the kicker is 380 mm for easy insertion in the beamline.

Design, manufacture and assemble of the kicker has been accomplished. Static field measurement using Hall probe was performed, and the integral field homogeneity is $\pm 0.3\%$ in good field region (± 30 mm). The commissioning of the pulsed power supply and dynamic field measurement using induction coil method is undergoing.

GANTRY BEAMLIN

For the gantry beamline, downstream scanning scheme was adopted to achieve larger field size and to avoid the use of large aperture dipole. The gantry beamline layout is shown

in Fig. 8, which includes two 57° dipoles (B1, B2), one 90° dipole (B3), six quadrupoles and one set of independent scanning magnets (ScMX, ScMY). A relative long SAD 2.8 m is adopted to compensate the skin dose effect due to non-parallel beam.

To provide stable beam size at the iso-center, an image optics was adopted for this gantry beamline [4]. Main fitting constraints are matching the first order transfer matrix R with $r_{11}, r_{22}, r_{33}, r_{44} \approx \pm 1$, and $r_{12}, r_{34} \approx 0$. In this condition, a

Content from this work may be used under the terms of the CC BY 3.0 licence (© 2019). Any distribution of this work must maintain attribution to the author(s), title of the work, publisher, and DOI

Content from this work may be used under the terms of the CC BY 3.0 licence (© 2019). Any distribution of this work must maintain attribution to the author(s), title of the work, publisher, and DOI

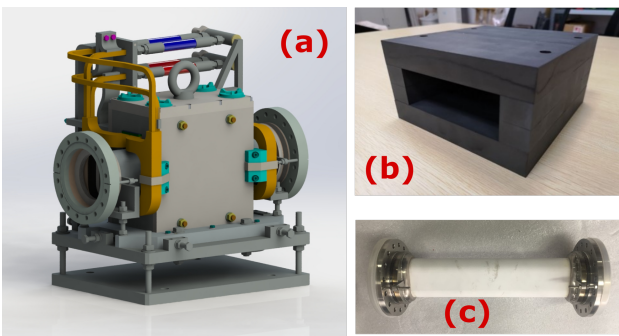


Figure 7: (a) Assemble view of the kicker magnet; (b) MnZn magnet core of the kicker; (c) Ceramic vacuum chamber.

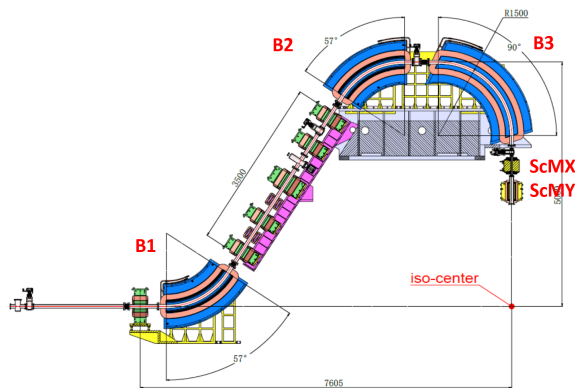


Figure 8: Gantry beamline with downstream scanning scheme.

nearly 1:1 magnification factor between the beam size at the iso-center and the initial beam size at CP can be formed.

The optics was firstly designed using Transport [2]. In order to investigate the high order aberrations and fringe field influence on beam optics, Cosy Infinity [3] and a self-developed ODE solver are used for validation. We fitted Enge function using realistic magnetic field extracted from OPERA-3D, then these Enge coefficients are used for optics optimization in Cosy Infinity. Minor changes on quadrupole strength (k) are required to maintain same beam condition at the iso-center. Figure 9 shows comparison of beam envelopes between Transport and first / second order results after optimization of Cosy Infinity. Study shows that the realistic fringe field has non-neglectable effect on beam optics, in terms of beam trajectory and dispersion function. However, second order aberration can be neglectable.

Detailed designs for all beamline elements including magnets, steerers, vacuum chamber and supports have been accomplished, by collaboration with Sigmaphi Accelerator Technologies. Figure 10 shows the final design for the quadrupole and 90° dipole.

CONCLUSION

Main design considerations and development progress for the beamline of HUST-PTF are introduced in this paper.

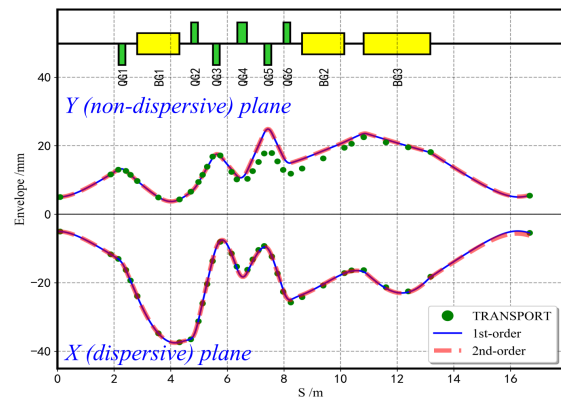


Figure 9: Comparison of 2σ beam envelope with Transport, first / second order results after optimization of Cosy Infinity.

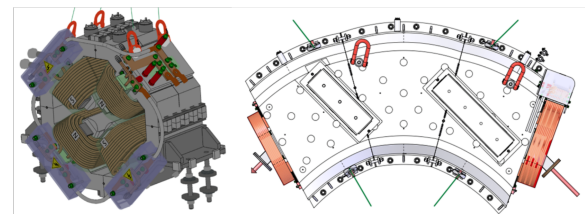


Figure 10: Detail design of quadrupole and 90° dipole.

Main beamline components have been designed and manufactured. Second order aberrations and fringe field effect has been considered, especially for the gantry beamline.

ACKNOWLEDGEMENTS

The authors would like to thank Lizhen Ma, Qinggao Yao and Wenjie Yang in Institute of Modern Physics, CAS, China, for their helps on design and field measurement of prototype magnets. They also thank Marie-Julie Leray and her group in Sigmaphi, for contributions on technical design of gantry beamline magnets.

REFERENCES

- [1] B. Qin *et al.*, “Progress of the beamline and energy selection system for HUST proton therapy facility”, in *Proceedings of IPAC 2017*, Copenhagen, Denmark, paper THPVA112.
- [2] U. Rohrer, PSI Graphic Transport Framework, based on a CERN-SLAC-FERMILAB version by K. L. Brown *et al.*, 2007. http://aea.web.psi.ch/Urs_Rohrer/MyWeb/trans.htm
- [3] M. Berz and K. Makino, “COSY INFINITY 10.0 Beam Physics Manual”, unpublished, August 2017.
- [4] B. Qin *et al.*, “Design of Gantry Beamline for HUST Proton Therapy Facility”, *IEEE Trans. on Appl. Supercond.*, vol. 28, pp. 1–5, 2018.
- [5] Z. Liang *et al.*, Design and optimization of an energy degrader with a multi-wedge scheme based on Geant4, *Nucl. Instr. Meth. A*, vol. 890, pp. 112–118, 2018.
- [6] Opera-3D reference, <http://www.operafea.com>